Paper No. 193, Bull. ISET, Vol. 16. No. 2, June 1979, pp. 63 - 74

# SOURCE MECHANISM OF TWO BURMA-INDIA BORDER EARTHQUAKES[1]

D.D. SINGH AND HARSH K. GUPTA[2]

## Introduction

Two strong earthquakes occurred in the Burma region. The USGS parameters for these two events are as follows :

(1) Date : October 17, 1969 ; Origin time ; 01 : 25 : 12.4 ; focal depth 134 km; epicentre 23.1°N, 94.7°E ; magnitude $m_b = 6.0$.

(2) Date : July 29, 1970 ; Origin time : 10 : 16 : 19 ; focal depth 59 km ; epicentre 26.0°N, 95 4°E ; magnitude $m_b = 6.5$.

Fault plane solution for the first event has been determined by Banghar (1974) and Chandra (1975) using first motion directions and S-polarization angles and by Das and Filson (1975) using first motion directions only. For the fault plane solution of the second event, Banghar (1974) and Chandra (1975) have used the body waves data and Rastogi (1976) has obtained the solution using both body and surface waves. Here we present the detailed study of fault plane solution and seismic source parameters from P, S and surface wave data.

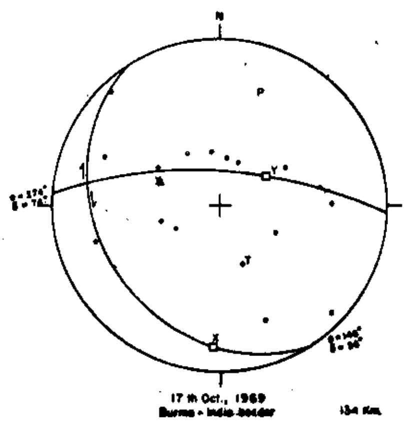


Fig. 1 Fault plane solution determined using first motions read from long-period records. Filled circles and open circles represent first-motion compressions and dilatations respectively. P is the pressure axis or axis of maximum compression, T is the tension axis or axis of least compression, X and Y are the poles of the two nodal planes

1 Paper No. 5 presented at Kurukshetra Symposium.

2 National Geophysical Research Institute, Hyderabad-7.

**Fault Plane Solution**

*First motion directions* Photocopies are prepared from the microfilms of 40 WWSSN stations. The first motion directions for these two earthquakes are read from the long-period vertical component of the records. These first motion directions are plotted on the lower hemisphere of the equal area projection. Figure 1 shows such plot for the first event.

Angles of incidence ($i_h$) are obtained from the extended distance (D) of Hodgson and Storey (1953) using the relation Cot $i_h = D$. The nodal planes are drawn separating the compression and dilatations. The azimuth, dip and slip angle for the two events are :

1. Plane a : $\theta = 326°$, $\delta = 26°$, $\lambda = 321°$

   Plane b : $\theta = 274°$, $\delta = 74°$, $\lambda = 288°$

2. Plane a : $\theta = 19°$, $\delta = 90°$, $\lambda = 298°$

   Plane b : $\theta = 110°$, $\delta = 28°$, $\lambda = 178°$

We have used the S-wave polarization data for defining these two nodal planes.

*S-wave polarization angles* The S-wave polarization angles are determined using the records of 25 WWSSN stations. Figure 2 shows the plot of observed S-polarization angles for the 1969 earthquake. The standard deviation and average error are calculated by varying the dip and strike of the nodal planes. These statistical parameters are least for the selected solution and these values are listed in Table 1 for the 1970 event.

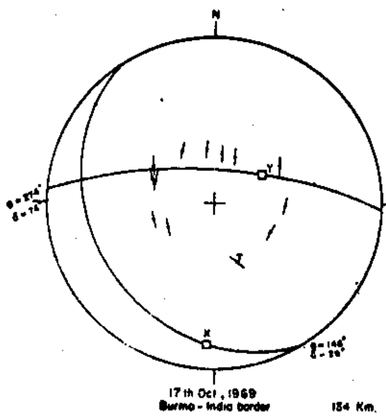


Fig. 2 Orientation of double-couple source from S-wave data. S-wave polarization directions are plotted by short lines

*Surface wave radiation pattern* In the fault plane solution determined with P and S, there is ambiguity in selecting the fault plane out of the two nodal planes. With the use of surface waves it is possible to define the fault plane as surface-waves amplitudes and initial phase have been shown to be dependent on azimuth and various source characteristics like depth, strike, dip and slip angle.

We have studied fundamental mode Rayleigh and Love waves. Photocopies of long-period vertical component seismograms are digitized for about six to eight minutes for the

**TABLE 1**

**Standard deviation and average error for different fault plane solution corresponding to our S-wave data of July 29, 1970 earthquake**

| Reference | Plane 1 S.D. | Plane 1 Average error | Plane 2 S.D. | Plane 2 Average error |
|---|---|---|---|---|
| This study and Chandra (1975) | 16.0 | 12.8 | 24 7 | 20.7 |
| Banghar (1974) | 32.4 | 28.1 | 32.4 | 28.1 |
| Das and Filson (1975) | 70.6 | 67.9 | 67.8 | 61.4 |
| Molnar et al. (1973) | 56.7 | 51.4 | 56.0 | 50.1 |

Rayleigh waves and three to five minutes of horizontal components (NS and EW) for Love wave, starting from the onset time. The digitization interval is taken to be 2.0 or 2.3 sec. The distribution of the stations covers the entire azimuth range. From the digitized data the mean and linear trend is removed. It is then Fourier analysed using the Simpson's method to get the amplitude and phase spectrum. These spectra are smooth using the Hamming and Tukey formula (Blackman and Tukey, 1958). The observed radiation pattern are obtained by plotting spectral amplitudes which are equalized at a certain distance. We have equalized at a distance of 36° using the relation

$$A_{ro} = \frac{A_r}{I} (\text{Sin } \Delta_1/\text{Sin } \Delta_2)^{1/2} \exp\left(\frac{\pi f (r_1 - r_2)}{Q U}\right)$$

where

$A_r$ = the observed amplitude spectra

$A_{ro}$ = the equalized spectral amplitude at a fixed distance

$I$ = the instrumental correction

$Q$ = the dissipation factor

$U$ = the group velocity

$\Delta_1$ and $r_1$ = the distance of the stations from the epicentre in degrees and kilomoters

$\Delta_2$ and $r_2$ = the equalized distance in degrees and kilometers (36° and 4000 km)

The Q values are taken from Ben-Menahem (1965) at periods greater than 50 sec and from Tsai and Aki (1969) at shorter periods. The instrumental correction is applied using the relation of Ben-Menahem et al. (1968).

The focal mechanism determination by the surface wave radiation pattern consists of comparing the observed radiation pattern with the theoretical one which is computed using the relation given by Ben-Menahem and Harkrider (1964) for various fault orientations at different time periods. This is an arduous process, because we have to test a large number of fault orientations by making different combinations of strike, dip and slip angles.

The theoretical radiation patterns are computed for both the nodal planes determined by other workers. In addition we tried some orientations close to these nodal planes in the ranges permitted from P wave data. The periods considered are 20, 40, 50, 62.5, 80 and 100 sec. The nodal plane 'a' mentioned earlier is giving the best fit and thus selected as the fault plane for these two events. The criteria for the selection of the best-fit solution is that the maximum number of observed points should fall near the periphery of the theoretical radiation patterns. Figure 3 shows the observed and theoretical radiation pattern for the 1970 earthquake. The scaling between the observed points and the theoretical curves are done visually. The scattering of the observed points in Figure 3 may be due to departures from the assumptions of simple layered media and point source model.

*Phase spectrum* Phase spectrum can also be used for the determination of the fault plane. The observed phase spectrum is equalized at the source using the relation of Udias and and Arroyo (1970). The theoretical phase spectra have been obtained for Rayleigh and Love waves with the method of Ben-Menahem and Harkrider (1964) for various fault plane orientations, which were considered earlier. The theoretical phase spectra are compared with the observed one at the source, for the time periods of 20, 40, 60 and 80 sec. The best fit solution obtained earlier are showing best fit with this data also (Figure 4).

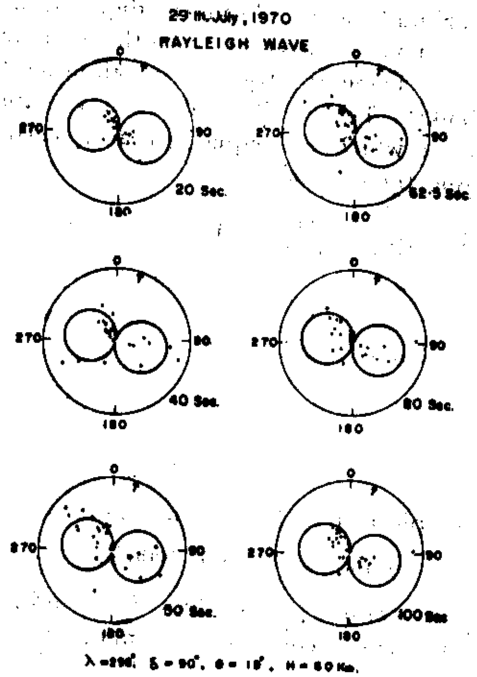


Fig. 3 (a) Comparison of observed fundamental - mode Rayleigh wave amplitudes (dots) with theoretical radiation pattern (best fit) computed at six time periods

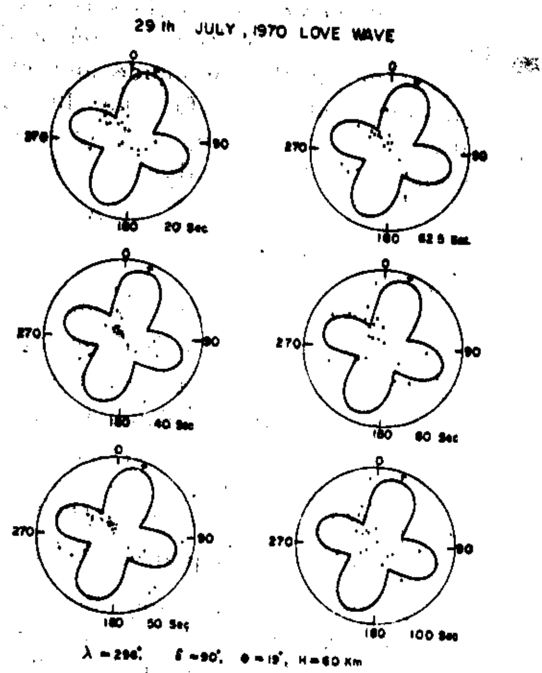


Fig. 3 (b) Comparison of observed fundamental-mode Love wave amplitudes (dots) with theoretical radiation pattern (best fit) computed at six time periods

## Direction of Rupture Propagation

Assuming the fracture to be represented by a line of point sources moving in one direction and using the directivity function of surface waves, we have determined the direction of rupture propagation. For this determination, we selected the stations in different

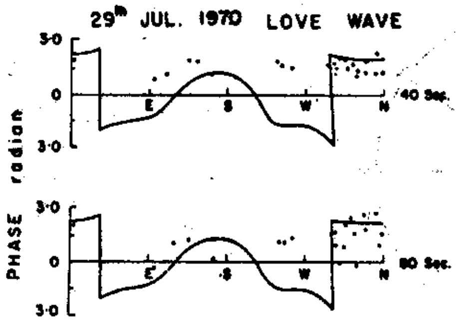


Fig. 4 Comparison of observed fundamental-mode Love wave phase spectrum (dots) with theoretical phase spectrum computed at two time periods

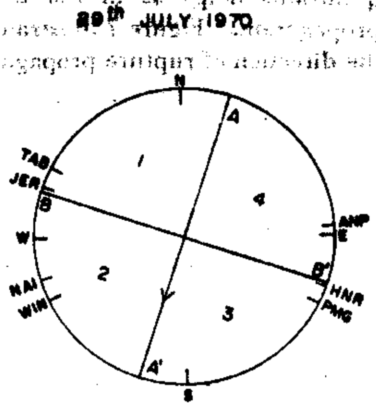


Fig. 5 Azimuthal location of the stations with respect to the strike of the fault plane. The arrow on the strike of the fault plane represents the direction of rupture propagation

azimuths such that they lie in four quadrants with respect to two nodal planes (Figure 5). The directivity function is determined at frequency interval of 0.005 Hz for four pair of stations (Figure 6) from the Rayleigh wave spectrum. For a pair of stations, the spectral amplitude for the second station is reduced to the distance of the first station and the ratio is taken using the amplitude value of the first station and this reduced amplitude as described by Singh et. al. (1975). The occurrence of the first maxima or minima at different

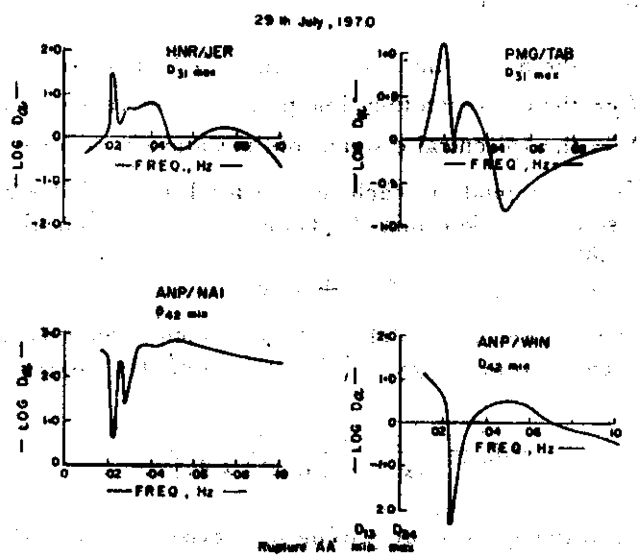


Fig. 6 Observed values of directivity function determined at different frequencies

quadrants helps us in the determination of the fault plane and the direction of rupture propagation. Figure 7 illustrates how it is possible. Using this method, we have determined the direction of rupture propagation to be southward along the fault plane.

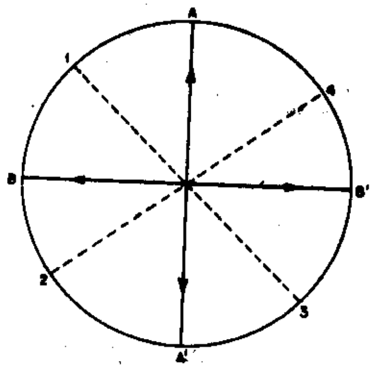


| RUPTURE | $D_{15}$ | $D_{24}$ |
|---|---|---|
| A'A | max | min |
| A A' | min | max |
| B'B | max | max |
| B B' | min | min |

Fig. 7 Maxima and minima of the directivity function and its relation to the direction of rupture propagation (after Udias, 1971)

**Source Parameters From Body Waves**

*Surface-wave magnitude and energy* The surface wave magnitude M is determined using the relation (Bath, 1966),

$$M = \log (A/T) + 1.66 \log \triangle + 3.30$$

where

A = the maximum ground amplitude in microns.

T = the corresponding time periods in the range of 18 to 22 sec.

$\Delta$ = the epicentral distance of the station in degrees.

The magnitude determined at each station are listed in Table 2 and 3. The seismic energy E at each station is determined (Table 2 and 3) from the magnitude using the relation (Richter, 1958).

$$\log E = 1.5 M + 11.8$$

*Seismic moment and apparent stress* The seismic moment from surface wave is determined using the relation (Udias and Arroyo, 1970) assuming the source time function to be a step function.

$$M_0 = \frac{| A_r | \ (2 \pi r)^{1/2}}{K_R \ N_{RZ} \ (h, \omega) \ | \ x(\theta) \ |}$$

where

$A_r$ = the spectral amplitude of Rayleigh wave at the recording station

r = the distance of the station from epicentre

$K_R$ = the wave number

**TABLE 2**

**Surface Wave Data, October 17, 1969**

| Station | Distance (deg) | Azimuth (deg) | ($10^{26}$ dyne—cm) Mo | M |
|---|---|---|---|---|
| MAT | 39.74 | 63 | 0.29 | 5.5 |
| TAB | 43.76 | 299 | 0.25 | 5.7 |
| JER | 52.96 | 291 | 0.19 | 5.8 |
| HLW | 56.50 | 291 | 0.18 | 5.6 |
| NUR | 60.37 | 327 | 0.47 | 5.8 |
| PMG | 60.64 | 118 | 0.26 | 5.4 |
| NAI | 61.27 | 254 | 0.08 | 5.7 |
| BUL | 77.45 | 241 | 0.36 | 5.8 |
| MBC | 78.70 | 08 | 0 82 | 5.6 |
| Average | | | 0.32 | 5.7 |

**TABLE 3**

Surface Wave Data, July 29, 1970

| Station | Distance (deg) | Azimuth (deg) | Mo ($10^{26}$ dyne-cm) | M | Energy release, E ($10^{21}$ ergs) |
|---|---|---|---|---|---|
| ANP | 23.59 | 86 | 2.28 | 6.0 | 0.63 |
| TAB | 42.82 | 299 | 2.65 | 6.0 | 0.63 |
| GUA | 47.98 | 95 | 2.03 | 6.4 | 2.51 |
| JER | 52.42 | 291 | 0.97 | 6.1 | 0.89 |
| IST | 56.07 | 303 | 1.97 | 6.0 | 0.63 |
| AAE | 56.14 | 203 | 9.07 | 6.5 | 3.55 |
| NUR | 58.25 | 327 | 4.88 | 6.6 | 5.01 |
| KEV | 58.36 | 338 | 4.97 | 6.1 | 0.89 |
| ATU | 60.60 | 301 | 3.77 | 6.2 | 1.26 |
| PMG | 61.42 | 118 | 4.73 | 6.0 | 0.63 |
| RAB | 62.63 | 110 | 1.34 | 6.3 | 1.78 |
| NAI | 62.64 | 254 | 0.22 | 6.4 | 2.51 |
| KBS | 63.39 | 348 | 5.73 | 6.5 | 3.55 |
| COP | 65.02 | 322 | 3.32 | 6.6 | 5.01 |
| NOR | 67.55 | 352 | 14.13 | 6.5 | 3.55 |
| ALE | 71.16 | 357 | 3.31 | 6.4 | 2.51 |
| HNR | 71.94 | 110 | 1.68 | 6.4 | 2.51 |
| ADE | 73.23 | 144 | 3.19 | 6.5 | 3.55 |
| ESK | 73.66 | 324 | 4.24 | 6.7 | 7.08 |
| VAL | 78.89 | 323 | 7.87 | 6.5 | 3.55 |
| RES | 79.32 | 3 | 5.05 | 6.0 | 0.63 |
| RIV | 79.67 | 136 | 5.38 | 6.5 | 3.55 |
| PRE | 82.00 | 238 | 2.25 | 6.3 | 1.78 |
| GDH | 82.35 | 349 | 13.28 | 6.7 | 7.08 |
| PTO | 83.00 | 312 | 8.23 | 6.4 | 2.51 |
| PDA | 95.00 | 316 | 9.09 | 6.6 | 5.01 |
| Average | | | 4.83 | 6.4 | 2.80 |

$x(\theta)$ = the radiation pattern function

$M_0$ = the seismic moment.

Using the spectral amplitude of Rayleigh wave for 50 sec. period for a number of stations the values of $M_0$ are calculated (Table 2 and 3).

The apparent stress is a measure of the stresses acting in the focal region of the earthquake. It can be written (Aki, 1966; Brune, 1968) as

$$\eta \bar{\sigma} = \mu \frac{E}{M_0}$$

where

$\eta$ = the seismic efficiency factor

$\bar{\sigma}$ = the average of the initial and final shear stress level on the fault

$\mu$ = the shear modulus

With the values of seismic moment and energy release obtained earlier, the apparent stress is estimated to be 2 bars for both the 1969 and 1970 earthquakes.

**Source Parameters From Body Waves**

*Seismic moment and source dimension* To determine the seismic moment and source dimension from teleseismic body-waves spectrum, we have selected 7 P-phases and 20 S-phases (horizontal components) of short and long-period records of 14 WWSSN stations. These P and S phases are digitized upto the sample length of 40 to 60 sec. The digitization interval for the short and long-period records are kept to be 0.306 and 0.96 sec., respectively. We have used the WILD A8-Autograph for digitization. The data were Fourier analyzed as described for surface waves. The resulting spectra are corrected for the effect of seismic attenuation by multiplying a factor of exp $(-\omega t/2\,Q)$, where t is the travel time of the waves. The Q values are taken from Julian and Anderson (1968). The resulting spectra are plotted on log-log graph paper. A few plots are shown in Figure 8 and the corresponding signals in Figure 9 for the event of 1970. The resulting spectra are approximated with a constant long-period spectral level $\Omega_0$, a spectral corner frequency $f_0$ and a high frequency spectral asymptote $f^{-\gamma}$. After getting these values, the seismic moment and source dimension are estimated using the relation.

$$M_0 = \frac{\Omega_0}{R_{\theta\phi}} 4 \pi \rho R v^3 \quad \text{(Keilis - Borok, 1959)}$$

$$r = \frac{2.34\, v}{2 \pi f_0} \quad \text{(Brune, 1970)}$$

where

$\rho$ = the density at the source

v = the wave velocity of the appropriate phase at the source

r = the radius of the circular source dimension

R = the term which accounts for the geometrical spreading in a flat stratified earth model

$R_{\theta\phi}$ = the radiation pattern function.

The average value of the seismic moment and source dimension is listed in table 4.

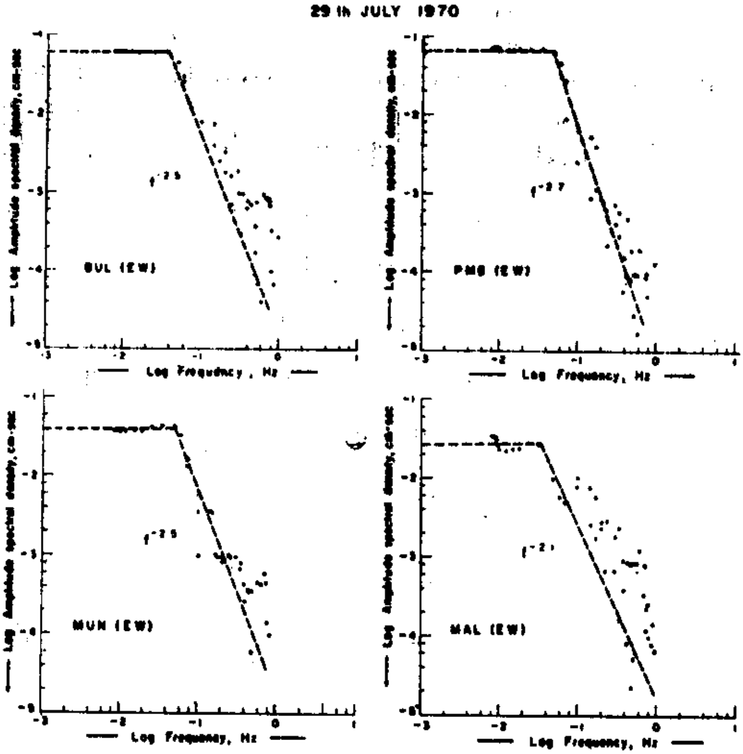


Fig. 8 Fourier amplitude spectra of short and long-period S-wave for some of the stations

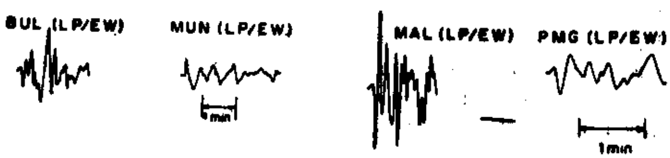


Fig. 9 Short and long-period S-waves recorded in the horizontal components

*Stress drop, dislocation and radiated energy* The stress drop of an earthquake is governed by the minimum tectonic stress and the material strength in the vicinity of the source region. We obtain the stress drop using the following relation (Brune, 1970) for a circular source model,

$$\Delta \sigma = \frac{7}{16} \frac{M_0}{r^3}$$

After getting the fault area $A = \pi r^2$ and seismic moment, the average dislocation across the fault plane is estimated using the relation

$$\bar{u} = \frac{M_0}{\mu A}$$

Using Brune's (1970) source model, the radiated energy, $E_R$ is estimated from the relation,

$$E_R = \frac{96\,\pi^3}{15\,R_{\theta\phi}^2}\,\rho\,v\,R^2\,f_0^3\left[\frac{2\gamma}{3\,(2\gamma-3)}\left(1-\frac{3\,(f_1/f_0)^{3-2\gamma}}{2\gamma}\right)\right]$$

where

$f_1$ = the highest frequency for the reliable spectral data.

All these source parameters are listed in Table 4.

**TABLE 4**

Source Parameter Estimates From Body Waves Spectra

| Event | Seismic moment $M_0$ ($10^{26}$ dyne-cm) | Source dimension r (km.) | Stress drop $\Delta\sigma$ (bars) | Average Dislocation $\bar{u}$ (cm.) | Radiated Energy $E_R$ ($10^{20}$ ergs) |
|---|---|---|---|---|---|
| 17 October, 1969 | 0.9 | 52 | 0.3 | 4 | $E_R(P)=1.79$ |
| 29 July, 1970 | 4.11 | 25.1 | 11 | 69 | $E_R(P)=7.19$ <br> $E_R(S)=1.35$ |

**Discussion**

The earthquake of July 29, 1970 occurred near the junction of the Himalayan and the Burmese mountain ranges. The mechanism solution for this event as inferred from surface wave indicates the near vertical north-north-east striking plane to be the fault plane which is consistent with the structural response results of Agrawal (1972). It gives a combination of normal faulting and right lateral strike-slip movement. The directions of rupture propagation is obtained to be southward. The earthquake of 1970 is possibly associated with some pre-existing NNE striking fault, the eastern side block of which is indicated to have moved southward. The northern tip of the nearby Mandalay fault has a NNE strike.

The earthquake of October 17, 1969 occurred in southern Burma at 23° latitude. The fault plane solution worked out for this event by us and other workers indicate thrust faulting. Unlike other events in Burma, the axis of pressure is parallel to the trend of the Burmese arc and thrusting direction is towards south. Out of the two nodal planes, the plane which strikes E-W is obtained to be the same by all the workers. The other shallow dipping plane is dipping southeast (Banghar, 1974; Chandra, 1975), south (Das and Filson, 1975) or southwest (present study). From surface wave we define the fault plane to have strike 146° and dip 26° SW. This fault shows thrust faulting and component of strike-slip movement. The directivity result shows that direction of rupture propagation is southward along the shallow dipping fault plane. This shows that earthquake may have resulted from the north-south compression caused by the southward underthrusting of the Burmese block or contortion of the descending lithosphere at a depth of 134 km.

## Conclusions

The focal mechanisms are obtained for two Burma-India Border earthquake using P-wave first motion directions, S-wave polarization angles and surface waves spectra. The 1969 earthquake indicates a combination of thrust and strike slip faulting along a plane with strike N 34° W; dip 26° SW and slip angle 321°. For the event of July 29, 1970 the fault plane is indicated to be near vertical and striking north-north-east. Direction of rupture propagation is southward along the fault plane as inferred from the directivity function.

The 1969 earthquake shows change in the direction of thrusting and may suggest the contortion in the descending lithosphere of the Indian plate at a depth of 134 km. The earthquake had a very low stress drop indicating that it may be due to movement on pre-existing fault.

## Acknowledgements

The authors are grateful to Dr. A. Roy, Director, National Geophysical Research Institute, Hyderabad, India for according permission to publish this work. We also wish to record our thanks to the Survey of India for access to the WILD-A8 Autograph and Electronics Corporation of India, Hyderabad for allowing us to use the computer.

## References

Agrawal, P.N., 1972. Structural response results during July 29, 1970 earthquake in Burma India border, Bull. Seism. Soc. Am. 62, 101-114.

Aki, K., 1966. Generation and propagation of G waves from the Niigata earthquake of June 16, 1964. Part 2. Estimation of earthquake moment, released energy, and stress-strain drop from the G-wave spectrum, Bull. Earthquake Res. Inst., Tokyo Univ. 44, 73-88.

Banghar, A.R., 1974. Mechanism of earthquakes in Albania, China, Mongolia, Afghanistan and Burma - India border, Earthquake Notes, Vol. XLV, No. 4, 13-25.

Bäth, M., 1966. Earthquake energy and magnitude, in Physics and Chemistry of the Earth, L.H. Ahrens, F.H. Press, K. Rankama and S.K. Runcorn, Editors, Pergamon, London, 7, 115-166.

Ben-Menahem, A., 1965. Observed attenuation and Q values of seismic surface waves in the upper mantel, J. Geophy. Res. 70, 4641-4651.

Ben-Menahem, A. & Harkrider, D.G., 1964. Radiation patterns of seismic surface waves from buried dipolar point sources in a flat stratified earth, J. Geophys. Res. 69, 2605-2620.

Ben-Menahem, A., Jarosch, H. & Rosenman, M., 1968. Large scale processing of seismic data in search of regional and global stress patterns, Bull. Seism. Soc. Am. 58, 1899-1932.

Blackman, R.B. & Tukey, J.W., 1958. The measurement of Power spectra, Dover, New York, 190 pp.

Brune, J.N., 1968. Seismic moment, seismicity, and rate of slip along major fault zones, J. Geophys. Res. 73, 777-784.

Brune, J.N., 1970. Tectonic stress and the spectra of seismic shear waves from earthquakes, J. Geophys. Res. 75, 4997-5009.

Chandra, U., 1975. Seismicity, earthquake mechanisms and Tectonics of Burma, 20°N - 28°N, Geophys. J. 40, 367-381.

Das, S. & Filson, J.R., 1975. On the tectonics of Asia, Earth and Planetary Science Letters, 28, 241-253.

Hodgson, J.H. & Storey, R.S., 1953. Tables extending Byerly's fault plane technique to earthquakes of any focal depth, Bull. Seism. Soc. Am. 43, 49-61.

Julian, B.R. & Anderson, D.L., 1968. Travel times, apparent velocities, and amplitudes of body waves, Bull. Seism. Soc. Am. 58, 339-366.

Keylis-Borok, V.I., 1959. An estimation of the displacement in an earthquake source and of source dimensions, Ann. Geofis. (Rome) 12, 205-214.

Molnar, P., Fitch, T.J. & Wu, F.T., 1973. Fault plane solutions of shallow earthquakes and contemporary tectonics in Asia, Earth and Planetary Science Letters, 19, 101-112

Rastogi, B.K., 1976. Source mechanism studies of earthquakes and contemporary tectonics in Himalaya and nearby regions, Bull. Int. Inst. Seism. Earthquake Eng., Tokyo 14, 99-134.

Richter, C.F., 1958. Elementary Seismology, W.H. Freeman, San Francisco, 768 pp.

Singh, D.D., Rastogi, B K. & Gupta, H.K., 1975. Surface wave radiation pattern and source parameters of Koyna earthquake of December 10, 1967, Bull. Seism. Soc. Am. 65, 711-731.

Tsai, Y. & Aki, K , 1969. Simultaneous determination of the seismic moment and attenuation of seismic surface waves, Bull. Seism. Soc. Am. 59, 275-287.

Udias, A., 1971. Source parameters of earthquakes from spectra of Rayleigh waves, Geophys. J. 22, 353-376.

Udias, A., & Arroyo, A.L., 1970. Body and surface wave study of source parameters of the March 15, 1964 Spanish earthquake, Tectonophysics 9, 323-346.